NASA TECHNICAL NOTE

NASA TN D-2193

NASA TN D-2193

EFFECTS OF LAMINAR-BOUNDARY-LAYER DISPLACEMENT ON A HEMISPHERE IN HELIUM FLOW

by Davis H. Crawford

Langley Research Center
Langley Station, Hampton, Va.

NATIONAL AERONAUTICS AND SPACE ADMINISTRATION • WASHINGTON, D. C. • APRIL 1964

EFFECTS OF LAMINAR-BOUNDARY-LAYER DISPLACEMENT ON A HEMISPHERE IN HELIUM FLOW

By Davis H. Crawford

Langley Research Center
Langley Station, Hampton, Va.

NATIONAL AERONAUTICS AND SPACE ADMINISTRATION

For sale by the Office of Technical Services, Department of Commerce,
Washington, D.C. 20230 -- Price $0.75

EFFECTS OF LAMINAR-BOUNDARY-LAYER DISPLACEMENT ON A HEMISPHERE IN HELIUM FLOW

By Davis H. Crawford

SUMMARY

Effects of laminar-boundary-layer displacement have been calculated for the hypersonic flow of helium over a hemisphere for stagnation Reynolds numbers from 10^3 to 2×10^5 and for ratios of wall to stagnation enthalpy of 1.0 and 0.1. The displacement effects were greatest for the hot-wall condition in the region near the shoulder and increased the heat transfer in this region as much as 50 percent. A comparison was made with estimated vorticity effects which gave a maximum increase in heat transfer in the stagnation region. In a hot-wall case for which vorticity increased the stagnation point heating rate by 1 percent, the heating rate at the 90° station was increased 20 percent because of displacement effect.

INTRODUCTION

Some recent investigations of the effects of second-order laminar boundary layer on the local aerodynamic and thermodynamic conditions on blunt bodies have assumed that displacement effects are negligible. This assumption is quite correct when cold-wall conditions are considered. (See refs. 1 and 2.) When the ratio of specific heats is near unity, the displacement effects are further overshadowed by other second-order effects. (See ref. 2.)

Hypersonic flight of vehicles in air is typical of flight in which displacement effects are often assumed to produce a negligible result on the flow over blunt bodies because the walls are cold (refs. 1 and 2), and because the real-gas effects (assuming equilibrium conditions) cause the ratio of specific heats to decrease and, at extreme conditions, to be near unity. There are, however, instances of gaseous flow in test cases for which the displacement effects are large in comparison with other second-order effects. For example, consider tests conducted in hypersonic helium tunnels where the model walls approach the free-stream stagnation temperature and where the ratio of specific heats is 5/3.

To determine the significance of the effects of boundary-layer displacement thickness, calculations of this thickness for helium flow over a hemisphere at hypersonic velocities have been effected by the use of the boundary-layer equations by a local similarity method with a Prandtl number of unity and with ratios of wall to stagnation enthalpy of 1.0 and 0.1. Subsequent calculations of the boundary-layer displacement thickness using the effective perturbations

of the surface inclination allowed convergence on a correct solution. The results of these calculations are correlated on the basis of a stagnation Reynolds number, and they utilize the stagnation conditions behind a normal shock.

SYMBOLS

A,B,C	empirical constants
a	velocity of sound
C_p	frozen specific heat at constant pressure
C_μ	coefficient in linear viscosity relation, $\frac{\mu}{\mu_\infty} = C_\mu \frac{T}{T_\infty}$
H	total enthalpy
h	local enthalpy
I	integral defined by equation (3)
M	Mach number
N_{Pr}	frozen Prandtl number
P,Q,R,N	parameters in correlating equations for transformed parameters
p	pressure
$\bar{q}$	local heat-transfer coefficient
R_∞	free-stream Reynolds number, $\frac{\rho_\infty u_\infty r}{\mu_\infty}$
R_e	modified Reynolds number used in reference 1, $\frac{\rho_t \sqrt{H}\, r}{\mu_t}$
$\tilde{R}$	modified Reynolds number, $\frac{\rho_t a_t r}{\mu_t}$
r	radius of hemisphere
T	temperature
t_w	ratio of wall enthalpy to free-stream total enthalpy
u	local velocity
β	velocity-gradient parameter defined by equation (4)
γ	ratio of specific heats

δ^* displacement thickness of boundary layer

δ^*_{tr} transformed displacement thickness (see ref. 3)

ϵ perturbation of surface inclination to correct for displacement effect

η similarity variable normal to surface

θ dimensionless stagnation enthalpy profile, $\frac{H - H_w}{H_e - H_w}$

Θ^*_{tr} transformed enthalpy thickness (see ref. 3)

θ^*_{tr} transformed momentum thickness (see ref. 3)

μ dynamic viscosity

ρ density

φ angle (station) measured from stagnation point on hemisphere

Subscripts:

e local stream conditions at outside edge of boundary layer

o wall condition in stagnation region without displacement effects

s wall condition at station of interest

t condition in stagnation region at outside edge of boundary layer

w wall conditions

∞ free-stream conditions ahead of model

A prime indicates differentiation with respect to the independent variable η.

METHOD OF CALCULATION

The laminar-boundary-layer displacement thickness and the local heat-transfer distribution have been calculated according to a method shown in reference 3. An integral method for the calculation of the laminar-boundary-layer parameters has been used. This method allows the previous history of the boundary layer to enter into the calculation of the pressure-gradient parameter and should therefore give more accurate results in the presence of a large pressure gradient. The assumption of local similarity satisfies the integral energy equation, and the boundary-layer profiles at each station are chosen from corresponding profiles from a family of similar solutions.

In order that the use of the method of reference 3 in machine computations be facilitated and that results be obtained in a form convenient for correlation, the forms of the equations were changed by the use of perfect-gas relations so that the displacement thickness and the heat-transfer distribution could be expressed in the following terms:

$$\frac{\delta^*}{r}\sqrt{\frac{R_\infty}{C_{\mu,t}M_\infty\frac{p_\infty}{p_t}\left(\frac{T_t}{T_\infty}\right)^{3/2}}} = \frac{p_t}{p_e}\left(\frac{C_{\mu,s}}{C_{\mu,t}}\frac{T_e}{T_t}\frac{I}{M_e^2}\right)^{1/2}\left[\frac{H_e}{h_e}\delta^*_{tr} + \left(\frac{H_e}{h_e} - 1\right)\theta^*_{tr} - \frac{H_e - H_w}{h_e}\Theta^*_{tr}\right] \tag{1}$$

For the displacement thickness in the stagnation region, equation (1) reduces to:

$$\frac{\delta^*}{r}\sqrt{\frac{R_\infty}{C_{\mu,t}M_\infty\frac{p_\infty}{p_t}\left(\frac{T_t}{T_\infty}\right)^{3/2}}} = \sqrt{\frac{C_{\mu,o}}{C_{\mu,t}}}\left\{2\left[\frac{d\left(\frac{u_e}{a_t}\right)}{d\varphi}\right]_t\right\}^{-1/2}\left[\delta^*_{tr} - \left(1 - t_{w,o}\right)\Theta^*_{tr}\right]_{\beta=1/2}$$

$$\frac{\bar{q}_s}{\bar{q}_o} = \frac{p_e}{p_t}\sqrt{\frac{C_{\mu,s}T_e}{C_{\mu,o}T_t}}\frac{\theta'_{w,s}}{\theta'_{w,o}}\frac{N_{Pr,o}}{N_{Pr,s}}\left\{2\left(\frac{I}{M_e^2}\right)\left[\frac{d\left(\frac{u_e}{a_t}\right)}{d\varphi}\right]_t\right\}^{-1/2} \tag{2}$$

in which

$$I = \frac{2}{\sin^2\varphi_s}\int_0^{\varphi_s}\frac{C_{\mu,w}}{C_{\mu,s}}\frac{p_e}{p_t}\frac{u_e}{a_t}\sin^2\varphi\, d\varphi \tag{3}$$

and where θ'_w, δ^*_{tr}, θ^*_{tr}, and Θ^*_{tr} are functions of β and t_w. These transformed parameters have been represented by simple relations and are presented in the appendix. The value of β may be determined as follows:

$$\beta = \frac{p_t}{p_e}\frac{I}{M_e^2}\left(\frac{T_t}{T_e}\right)^2\frac{d\left(\frac{u_e}{a_t}\right)}{d\varphi}\frac{C_{p,t}}{C_{p,e}} \tag{4}$$

Examination of the relation for δ^* (eq. (1)) shows that the quantities on the right-hand side of this equation may be completely determined from the local conditions. These quantities become independent of the free-stream Mach number at hypersonic velocities because of the Mach number "freeze." The quantity on the left-hand side of this equation represents δ^*/r multiplied by the square root of a modified Reynolds number. This modified Reynolds number is observed to be a function only of the free-stream flow quantities, but with the aid of perfect-gas relations it can be shown to be a function only of stagnation conditions. That is,

$$\tilde{R} = \frac{R_\infty}{C_{\mu,t} M_\infty \frac{p_\infty}{p_t}\left(\frac{T_t}{T_\infty}\right)^{3/2}} = \frac{\rho_t a_t r}{\mu_t} \tag{5}$$

In this form, the Reynolds number is related to the Reynolds number used in reference 1 by a constant factor, as follows:

$$\tilde{R} = \sqrt{\gamma - 1}\, R_e$$

The value of C_μ for helium is not a function of absolute temperature as it is for air; therefore, $\tilde{R}$ is a function of M_∞ and R_∞. Thus, it is possible to evaluate $\tilde{R}$ to determine the displacement effects directly from one of a family of curves, such as shown in figure 1.

From a predetermined pressure distribution, the local flow conditions just outside the boundary layer were calculated by assuming isentropic flow from the stagnation point. From the local flow conditions, I, β, $\bar{q}_s/\bar{q}_o$, and $\frac{\delta^*}{r}\sqrt{\tilde{R}}$ were calculated at stations 1^o apart on the hemisphere. The growth of the boundary-layer displacement thickness was assumed as a perturbation of the original surface, a correction angle $\left(\epsilon = \arctan \frac{1}{r}\frac{d\delta^*}{d\varphi}\right)$ was added at each station, and the entire calculation was repeated as an iteration on the original results.

As a trial, the pressure distribution was assumed to be given by a modified Newtonian-Prandtl-Meyer theory. This pressure distribution and its first derivative were continuous, but its second derivative had a discontinuity at the match point. (See refs. 4 and 9.) This discontinuity caused calculations downstream of the match point to be in error after the initial calculation and to diverge wildly after subsequent iterations.

After the necessity of expressing the local conditions on the surface of the sphere as a continuous function of the surface inclination to the free stream became apparent, the local Mach number was considered the best parameter to express as an empirical continuous function. A function of the form

$$M_e = A\varphi + B\varphi^2\left(1 - \cos\frac{\pi}{2}\varphi\right) + C\sin^3\left(\frac{\pi}{2}\varphi\right)$$

was chosen to represent the shape of the Mach number distribution. The constants were chosen to represent the Mach number distribution near the stagnation point predicted by the theory of reference 5 for $M_\infty = \infty$ and to fit data near the shoulder of a hemisphere-cylinder from reference 6. The equation used in the calculations for helium was

$$M_e = 1.20\varphi + 0.210\varphi^2\left(1 - \cos\frac{\pi}{2}\varphi\right) + 0.050\sin^3\left(\frac{\pi}{2}\varphi\right)$$

Even with the local flow conditions outside the boundary layer expressed as a continuous function of surface inclination, the repeated calculations of the boundary-layer parameters did not converge well, especially at low Reynolds numbers and for stations near the shoulder. The calculated values of ϵ as a function of φ often developed a continuously fluctuating appearance near the shoulder, and cumulative errors caused some scatter to appear in the values of ϵ. At this point, further iteration was hopeless without some smoothing of the values of ϵ. This smoothing was accomplished by a machine program which gave the best root-mean-square fit to selected values of ϵ, and further calculations were made using these smoothed values. When the output correction angles repeated the input correction angles accurately, the computation was considered complete.

RESULTS AND DISCUSSION

The displacement thickness calculated in this investigation is shown in figure 2. It is apparent that wall enthalpy plays an important part in the determination of the displacement thickness. In the stagnation region the displacement thickness is reduced to a negative value when the wall temperature is as low as one-tenth the free-stream stagnation temperature. In the shoulder region, the displacement thickness is reduced an order of magnitude as the value of t_w is reduced from 1.0 to 0.1. Also shown in figure 2 is the boundary-layer displacement effect upon the boundary-layer displacement thickness. If there were no displacement effect, $\frac{\delta^*}{r}\sqrt{\tilde{R}}$ would not be a function of $\tilde{R}$.

As a direct consequence of the boundary-layer displacement, the effective surface inclination is slightly different from the actual surface inclination. This effective perturbation of the surface inclination ϵ is shown in figure 3 as a function of modified Reynolds number $\tilde{R}$. With no displacement effects, $\frac{1}{r}\frac{d\delta^*}{d\varphi}$ is inversely proportional to the square root of $\tilde{R}$. For small angles, $\epsilon = \arctan \frac{1}{r}\frac{d\delta^*}{d\varphi} \approx \frac{1}{r}\frac{d\delta^*}{d\varphi}$ follows the same rule very closely. The large deviation from this rule, as shown in figure 3(a), is caused by the displacement effect upon growth of the boundary layer. As expected, the displacement effect is greater for larger values of ϵ. Comparison of figures 3(a) and 3(b) shows the smaller perturbation angles in figures 3(a) and the smaller displacement effect on these angles which is realized with the cold wall (fig. 3(b)).

The change in effective surface inclination caused by the increase in the boundary-layer displacement thickness directly affects the pressure distribution. This effect of boundary-layer displacement on surface pressures at a number of stations is shown in figure 4. Since the growth of the boundary-layer displacement thickness is much less for the cold wall than for the hot wall, the displacement effect on the pressures is also much less. The pressure at the shoulder has been doubled by the displacement effect at lower values of the Reynolds number for $t_w = 1.0$. The displacement thickness and the growth of the displacement thickness decrease toward the stagnation point, and thus the displacement effect on the surface pressures is a maximum at the shoulder of the hemisphere-cylinder and decreases toward the stagnation point.

An experimental check on the validity of these calculated results is possible by comparison of the calculated Reynolds number effect on the shoulder pressure of a hemisphere-cylinder with that found experimentally in helium tunnel tests. (See ref. 7.) Calculations made at a Mach number of 18 were compared with data taken in a range of Mach numbers from 15.6 to 21. The data and calculations were compared in a range of free-stream Reynolds numbers from approximately 0.01×10^6 to 0.40×10^6. This comparison is shown in figure 5, and the agreement between the calculated and experimental results is good in this range of flow conditions.

Through the change in the local pressure distribution, the local Mach number distribution is reduced by the boundary-layer displacement effect. This displacement effect on the local Mach number distribution is shown in figure 6. The Mach number resulting from the inviscid calculation is shown compared with the Mach number calculated with the displacement effects at two Reynolds numbers. In the determination of the constants used in the empirical expression for the Mach number distribution for the assumed inviscid case, the higher values of the data from references 6, 8, and 9, as given in reference 6, were purposely favored. The calculation of M_e for $\tilde{R} = 1.2 \times 10^4$ appears to be a better fit with the data than the assumed inviscid relation, especially when the Reynolds numbers of the individual data points are considered. The calculation at $\tilde{R} = 1.2 \times 10^3$ shows the local Mach number distribution for the lowest Reynolds number considered for calculation and, thus, for the greatest displacement effect.

The displacement effect on the pressure distribution directly affects the heat-transfer-coefficient distribution. The values of $\bar{q}_s/\bar{q}_o$ are presented in figure 7. This manner of presentation of the heat transfer is selected because the Prandtl number has been shown to have little effect on the heat-transfer distribution. (See ref. 3.)

Again, the displacement effect is seen to be much greater for the hot wall. At the low Reynolds number considered, the value of $\bar{q}_s/\bar{q}_o$ is increased slightly more than 50 percent at the shoulder ($\varphi = 90°$). This increase is greater than the value expected from a consideration of the square root of the pressure. (See ref. 10.) Thus the heat-transfer coefficient has been increased beyond that expected from the pressure increase by the presence of a less favorable pressure gradient.

Values of $\frac{d\left(\frac{u_e}{a_t}\right)}{d\varphi}$ are shown in figure 8 to facilitate the study of possible displacement effects on the heat transfer in the stagnation region. For comparison, the values of this parameter are shown for other stations. For the hot wall $\left(t_w = 1.0\right)$, the variation in $\frac{d\left(\frac{u_e}{a_t}\right)}{d\varphi}$ with $\tilde{R}$ is about 3 percent throughout the range of Reynolds numbers considered, and the laminar-heat-transfer coefficient in the stagnation region varies with the square root of the velocity gradient. Thus, it is obvious that at these Reynolds numbers the displacement effect on the heat transfer in the stagnation region is small.

In hypersonic flow at very low Reynolds numbers, the detached curved shock ahead of a blunt body induces vorticity in the flow between the shock and the wall. This vorticity effect is shown in figure 9 in comparison with the displacement effect. In contrast with the displacement effect which reaches a maximum at the shoulder, the vorticity effect reaches a maximum in the stagnation region.

The displacement effect is often neglected in calculations of vorticity or second-order boundary-layer effects. Such calculations are for a cold wall, however, and it has previously been shown in this report that the displacement effect becomes small for a cold wall. Comparison of the displacement and vorticity effects for a cold wall ($t_w = 0.1$) are shown in figure 9 for $\tilde{R} = 1.2 \times 10^3$. Here, it is seen that from the standpoint of percentages the maximum displacement effect is comparable to the maximum vorticity effect.

When the wall is hot, as it is in many helium tests, the displacement effect is greater, whereas the vorticity effect is unchanged. Then the displacement effect cannot be neglected except, perhaps, in the stagnation region. A comparison of the approximate vorticity effect predicted in reference 1 with the displacement effect at $\tilde{R} = 1.2 \times 10^3$ is shown in the center portion of figure 9. Here, the displacement effect overshadows the vorticity effect at stations away from the stagnation region. Other second-order theories (ref. 2) show heat-transfer increases smaller than those shown in reference 1. The displacement effect on the heat-transfer coefficient with $\tilde{R} = 10^4$ is also shown in figure 9. In this case, the vorticity effect does not appear in the figure since it has a maximum value of about 1 percent, whereas the maximum displacement effect was approximately 20 percent at the 90° station of a hemisphere.

CONCLUDING REMARKS

The boundary-layer displacement thickness has been calculated for the hypersonic flow of helium over a hemisphere by the application of solutions of the boundary-layer equations by a local similarity method with a Prandtl number of 1. The calculations included a range of modified Reynolds numbers from 10^3 to 2×10^5 and ratios of wall to stagnation enthalpy of 0.1 and 1.0. Close agreement was seen between an experimentally determined and a calculated displacement effect on the shoulder pressure for a hemisphere-cylinder.

This calculated boundary-layer displacement effect on the heat transfer and pressure distribution has been correlated in a fashion which is easy to apply. The displacement effect was small at the stagnation point but increased at stations more distant from the stagnation point. For the hot wall, the effects of the boundary-layer displacement thickness became significant as the shoulder region was approached. The heat transfer was increased in this region to a value as much as 50 percent greater than for the inviscid case. This result is in sharp contrast to that for the cold wall where the displacement effect on the heat transfer is an order of magnitude lower.

The calculated displacement effect was compared with the second-order effect by vorticity as given in PIBAL Report No. 611. This vorticity effect was a maximum in the stagnation region and decreased toward the shoulder. In the case of the hot wall, at a modified Reynolds number of 1.2×10^3 the maximum boundary-layer displacement effect which occurs in the shoulder region causes a much greater percent increase in the heat transfer than does the maximum vorticity effect which occurs in the stagnation region. At this same Reynolds number, but with a cold wall, the maximum percent increase in the heat transfer caused by the displacement effect was approximately the same as that caused by the vorticity effect. At a modified Reynolds number of 10^4, the maximum vorticity effect was approximately 1 percent in the stagnation region and the maximum displacement effect for a hot wall was approximately 20 percent at the 90° station of the hemisphere.

Langley Research Center,
National Aeronautics and Space Administration,
Langley Station, Hampton, Va., November 21, 1963.

APPENDIX

CORRELATING EQUATIONS FOR THE TRANSFORMED PARAMETERS

These correlating equations were determined by the method outlined in reference 3. From these equations, the transformed parameters δ^*_{tr}, θ^*_{tr}, Θ^*_{tr}, and θ'_w may be calculated for values of β from 0 to about 6.

$$\delta^*_{tr} = \left(0.9793 - 0.4142t_w + 0.0828t_w^2\right)\frac{1 + P\beta^{0.85}}{Q + R\beta^{0.85}}$$

where

$$P = 0.494065 - 0.468441t_w + 0.096926t_w^2$$

$$Q = 0.804816 - 0.340402t_w + 0.068048t_w^2$$

$$R = 0.689249 - 0.128035t_w + 0.028874t_w^2$$

$$\theta^*_{tr} = \left(0.4033 - 0.1054t_w - 0.0056t_w^2\right)\frac{1 + P\beta^{0.95}}{Q + R\beta^{0.95}}$$

where

$$P = 0.82683 - 0.84672t_w + 0.16412t_w^2$$

$$Q = 0.85882 - 0.22447t_w - 0.0119t_w^2$$

$$R = 0.96801 - 0.62225t_w + 0.17602t_w^2$$

$$\Theta^*_{tr} = \left(1.1371 - 0.1455t_w + 0.0346t_w^2\right)\frac{1 + P\beta^{0.88}}{Q + R\beta^{0.88}}$$

where

$$P = 0.68670 + 0.04027t_w + 0.07862t_w^2$$

$$Q = 0.93442 - 0.11955t_w + 0.02842t_w^2$$

$$R = 0.75228 + 0.15982t_w + 0.05020t_w^2$$

$$\theta_w' = \left(5.0667 + 0.07776t_w - 0.01396t_w^2\right)\frac{1 + P\beta^N}{Q + R\beta^N}$$

where

$$P = 0.564 + 0.022t_w + 0.168t_w^2$$

$$Q = 1.079 + 0.164t_w - 0.028t_w^2$$

$$R = 0.485 - 0.146t_w + 0.200t_w^2$$

and

$$N = 0.699 - 0.128t_w + 0.072t_w^2$$

REFERENCES

1. Ferri, Antonio, Zakkay, Victor, and Ting, Lu: Blunt Body Heat Transfer at Hypersonic Speed and Low Reynolds Numbers. PIBAL Rep. No. 611 (ARL Tech. Note 60-140), Polytechnic Inst. Brooklyn, June 1960.

2. Van Dyke, Milton: Second-Order Compressible Boundary-Layer Theory With Application to Blunt Bodies in Hypersonic Flow. SUDAER No. 112 (AFOSR-TN-61-1270), Stanford Univ., July 1961.

3. Beckwith, Ivan E., and Cohen, Nathaniel B.: Application of Similar Solutions to Calculation of Laminar Heat Transfer on Bodies With Yaw and Large Pressure Gradient in High-Speed Flow. NASA TN D-625, 1961.

4. Lees, Lester, and Kubota, Toshi: Inviscid Hypersonic Flow Over Blunt-Nosed Slender Bodies. Jour. Aero. Sci., vol. 24, no. 3, Mar. 1957, pp. 195-202.

5. Van Dyke, Milton D., and Gordon, Helen D.: Supersonic Flow Past a Family of Blunt Axisymmetric Bodies. NASA TR R-1, 1959.

6. Bertram, Mitchel H., and Everhart, Philip E.: An Experimental Study of the Pressure and Heat-Transfer Distribution on a 70° Sweep Slab Delta Wing in Hypersonic Flow. NASA TR R-153, 1963.

7. Bertram, Mitchel H., and Henderson, Arthur, Jr.: Recent Hypersonic Studies of Wings and Bodies. ARS Jour., vol. 31, no. 8, Aug. 1961, pp. 1129-1139.

8. Vas, I. E., Bogdonoff, S. M., and Hammitt, A. G.: An Experimental Investigation of the Flow Over Simple Two-Dimensional and Axial Symmetric Bodies at Hypersonic Speeds. Rep. No. 382 (WADC TN 57-246), Dept. Aero. Eng., Princeton Univ., June 1957.

9. Wagner, Richard D., Jr., Pine, W. Clint, and Henderson, Arthur, Jr.: Laminar Heat-Transfer and Pressure-Distribution Studies on a Series of Reentry Nose Shapes at a Mach Number of 19.4 in Helium. NASA TN D-891, 1961.

10. Bertram, Mitchel H., and Feller, William V.: A Simple Method for Determining Heat Transfer, Skin Friction, and Boundary-Layer Thickness for Hypersonic Laminar Boundary-Layer Flows in a Pressure Gradient. NASA MEMO 5-24-59L, 1959.

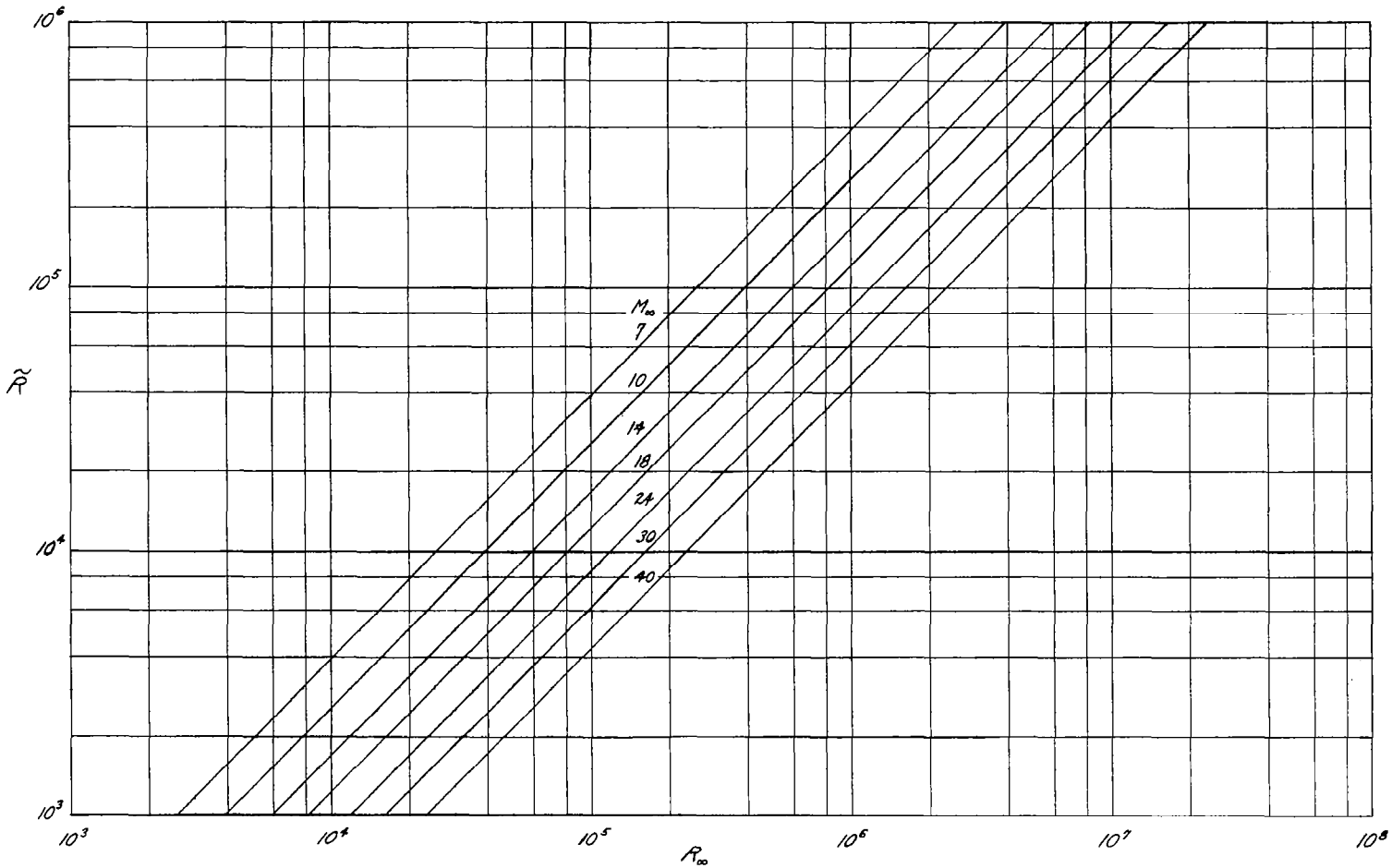

Figure 1.- Curve for determination of stagnation Reynolds number for various free-stream Mach numbers and Reynolds numbers in helium flow.

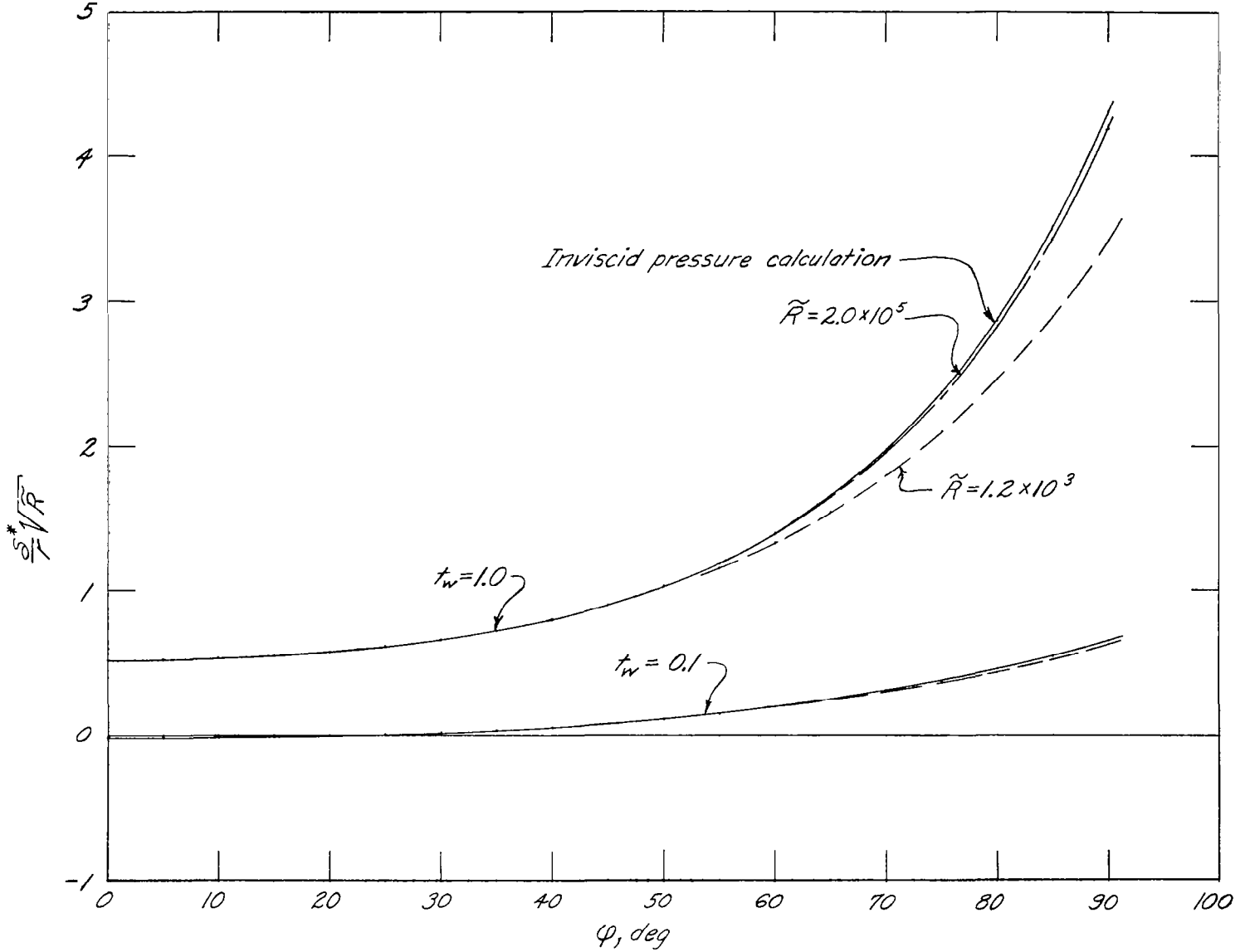

Figure 2.- Boundary-layer displacement effect upon boundary-layer displacement thickness.

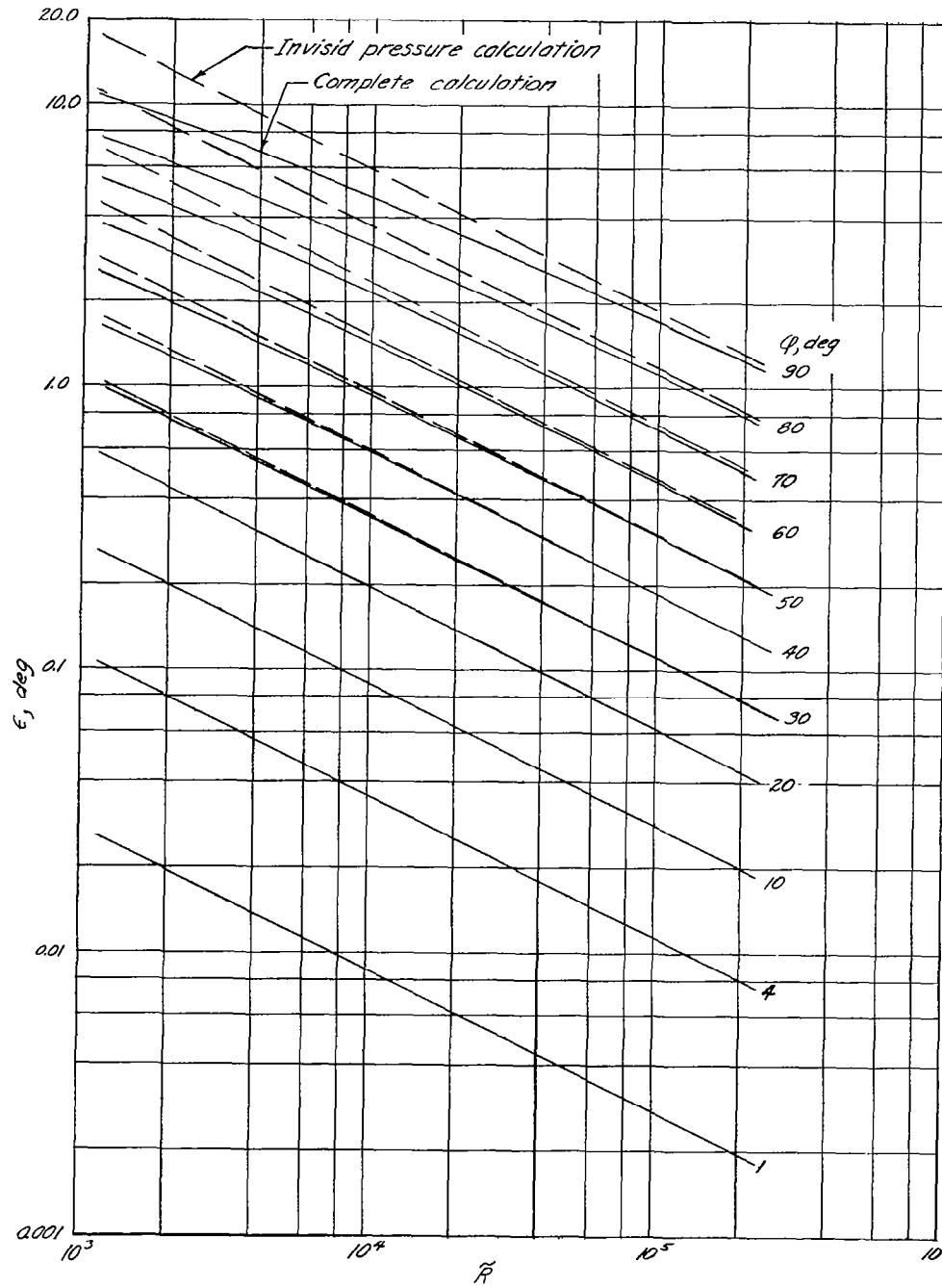

(a) $t_w = 1.0$.

Figure 3.- Boundary-layer displacement perturbation of effective surface inclination to the airstream.

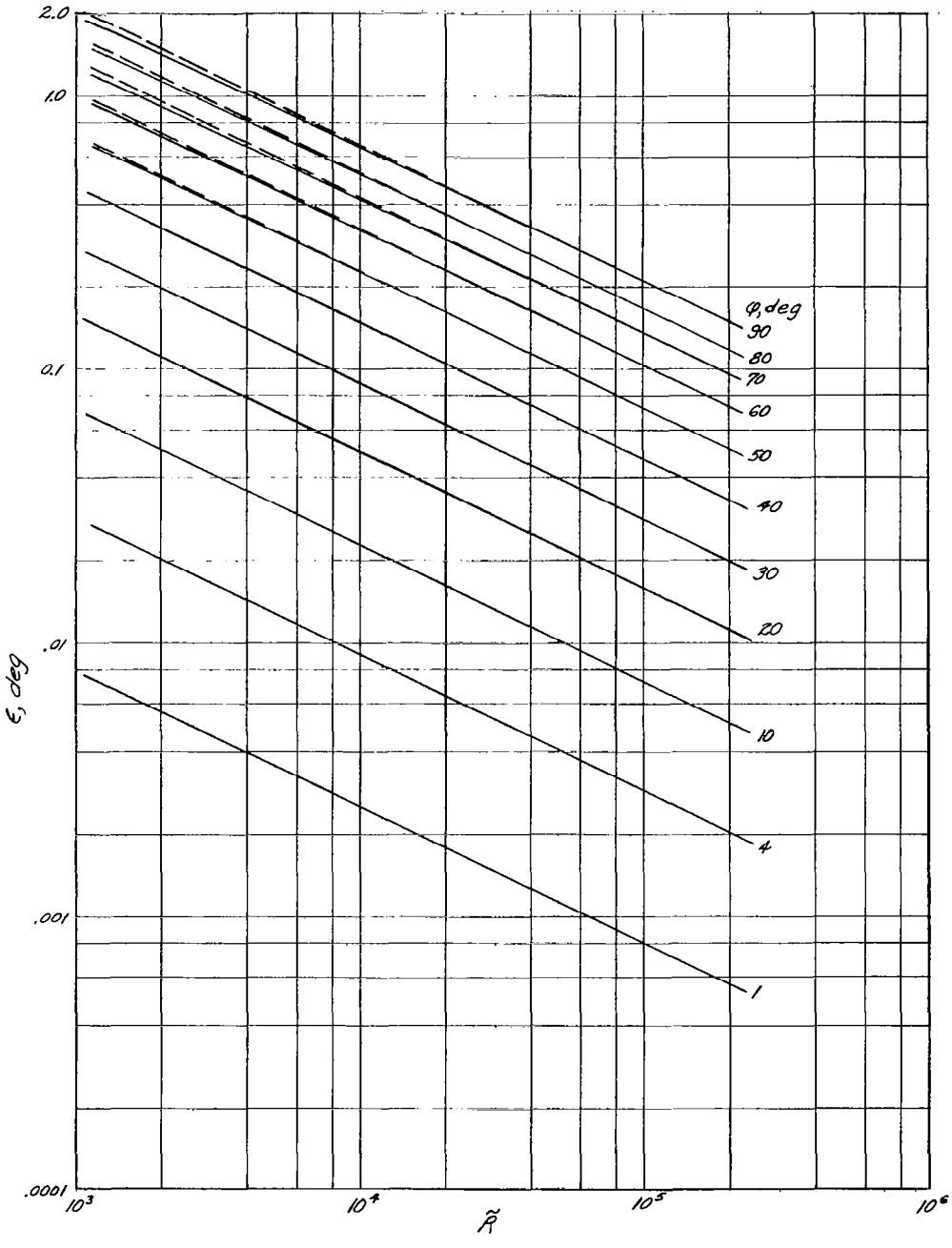

(b) $t_w = 0.1$.

Figure 3.- Concluded.

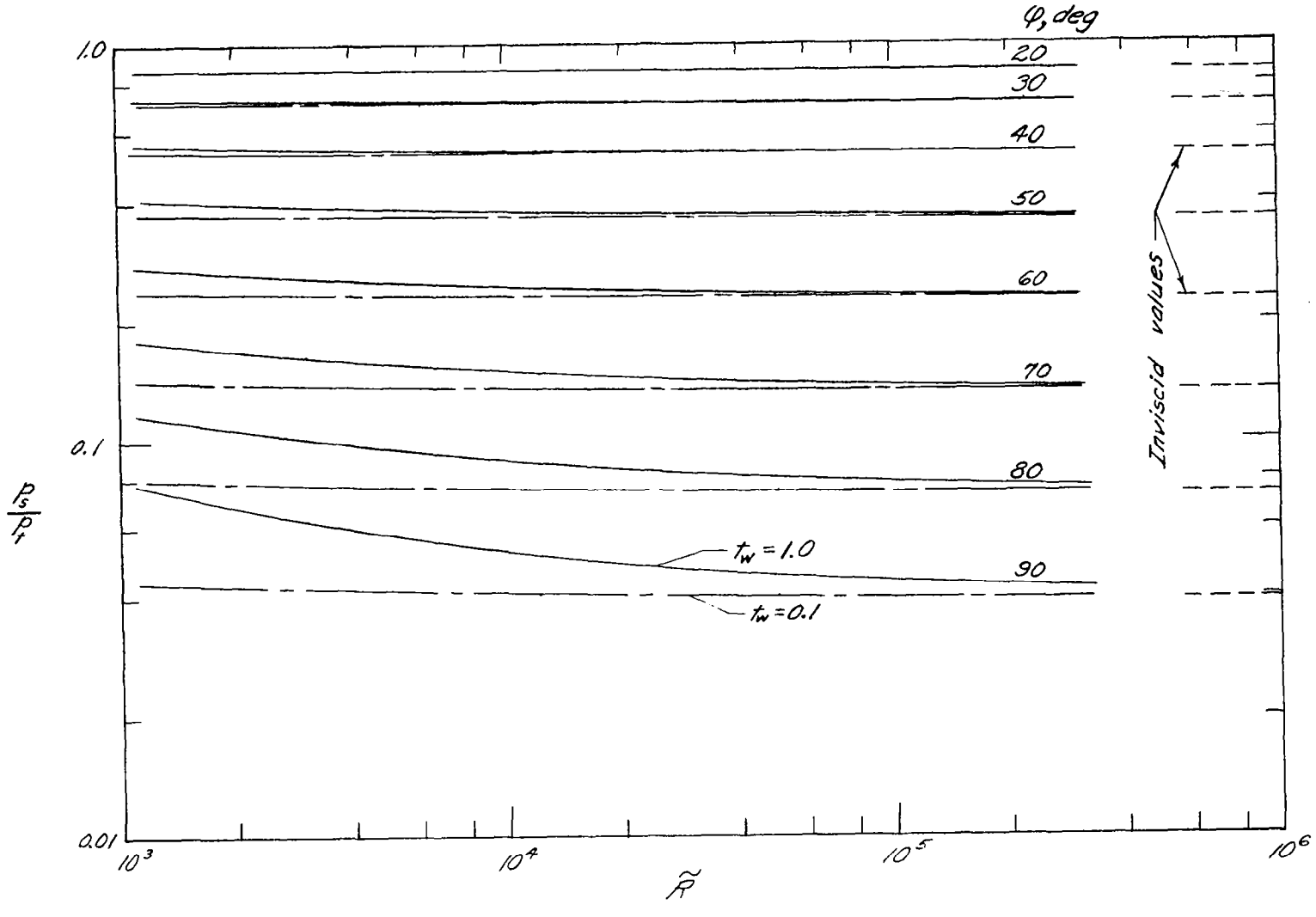

Figure 4.- Calculated displacement effect on surface pressure at various stations on a hemisphere.

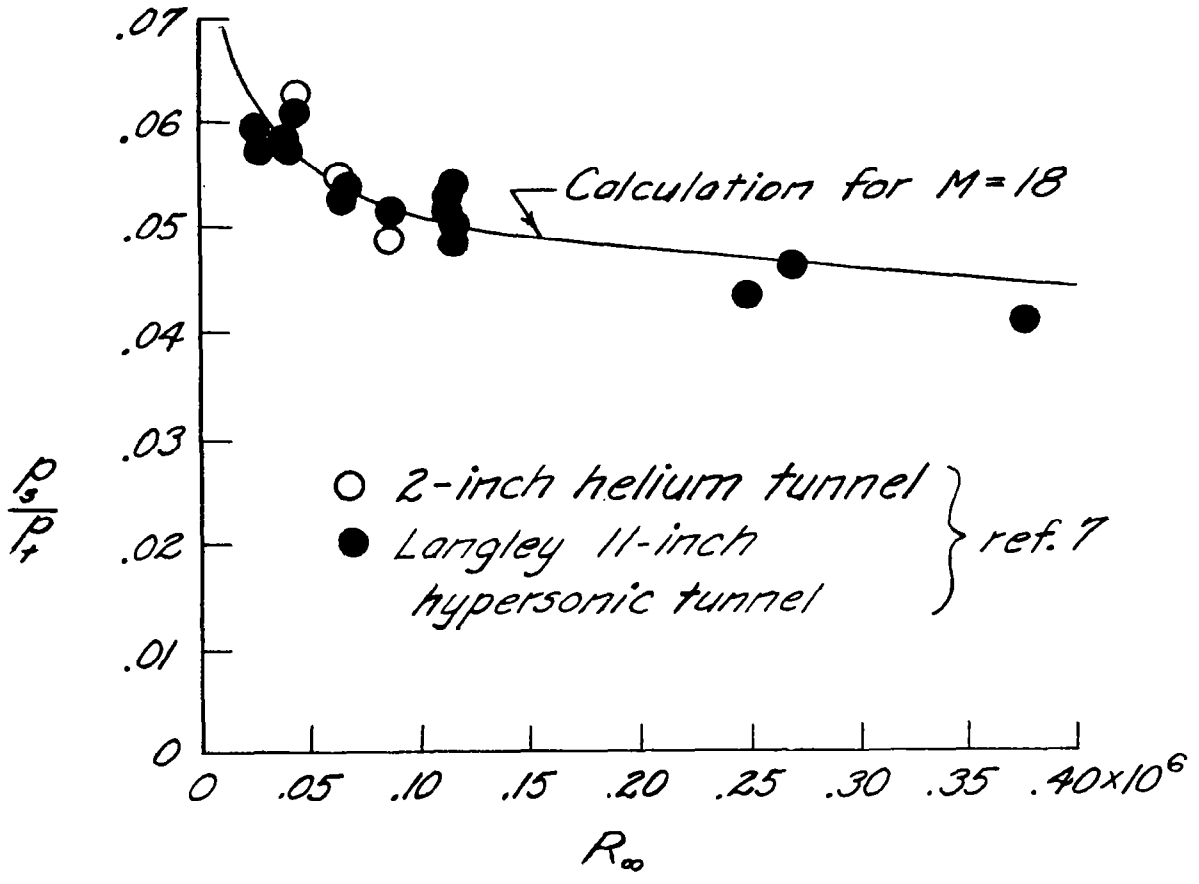

Figure 5.- Experimental Reynolds number effect on hemisphere-cylinder shoulder pressure compared with calculated displacement effect. ($15.6 \leq M_\infty \leq 21.$)

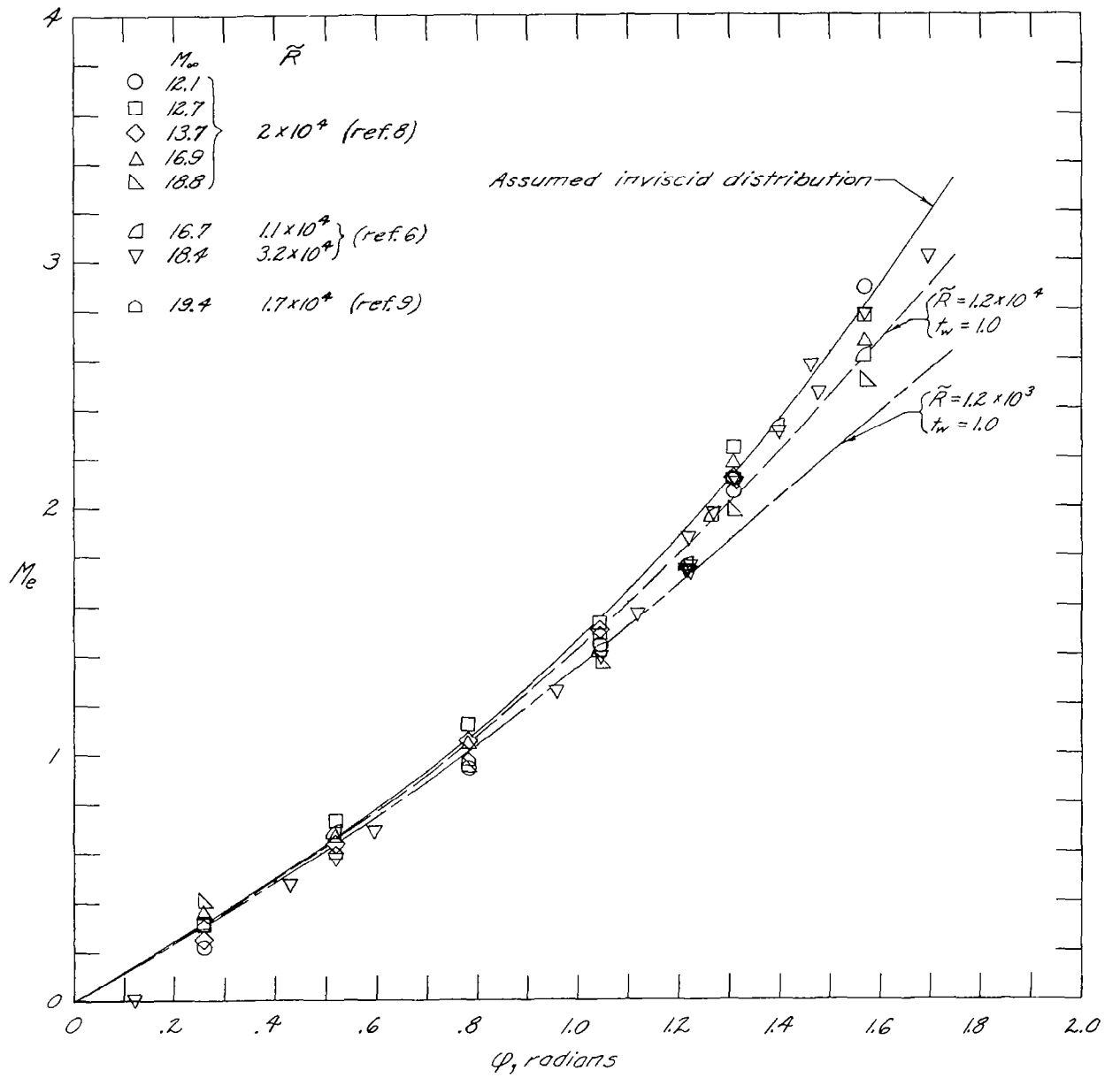

Figure 6.- Local Mach number distribution for helium flow over hemisphere.

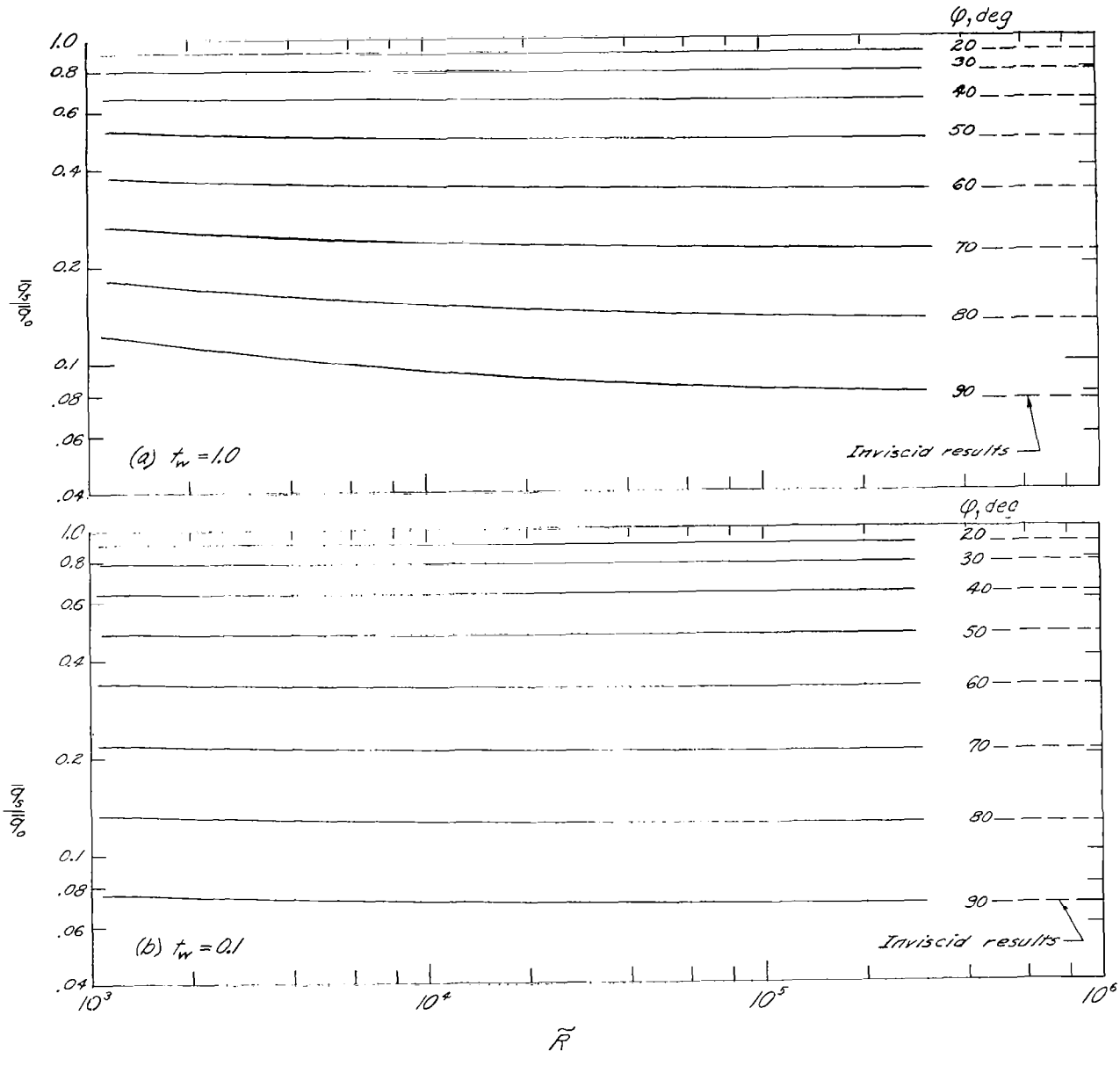

Figure 7.- Boundary-layer displacement effect on heat-transfer coefficient distribution.